Palaeogeography, Palaeoclimatology, Palaeoecology 313-314 (2012) 150–161

Contents lists available at SciVerse ScienceDirect

Palaeogeography, Palaeoclimatology, Palaeoecology

journal homepage: www.elsevier.com/locate/palaeo

Paleogene temperature gradient, seasonal variation and climate evolution of northeast China

Cheng Quan [a,b,c,*], Yu-Sheng (Christopher) Liu [c,*], Torsten Utescher [d,e]

[a] Research Center of Paleontology and Stratigraphy, and Key Laboratory for Evolution of Past Life and Environment in Northeast Asia, Jilin University, Changchun, Jilin 130026, China
[b] State Key Laboratory of Palaeobiology and Stratigraphy, Nanjing Institute of Geology and Palaeontology, Chinese Academy of Sciences, Nanjing, Jiangsu 210008, China
[c] Department of Biological Sciences, and Don Sundquist Center of Excellence in Paleontology, Box 70703, East Tennessee State University, Johnson City, Tennessee 37614, USA
[d] Steinmann Institute, Bonn University, Bonn 53115, Germany
[e] Senckenberg Research Institute, Frankfurt 60325, Germany

ARTICLE INFO

Article history:
Received 31 March 2011
Received in revised form 26 October 2011
Accepted 30 October 2011
Available online 7 November 2011

Keywords:
Paleogene climate evolution
Climatic seasonality
Temperature gradient
Quantitative reconstruction
Eocene cooling
Northeast China

ABSTRACT

Continental Paleogene climates have been well studied in Europe and North America, but very little is known from Asia because paleoclimatic results have only been reported from particular geological intervals. Here, based on 29 plant assemblages from 8 well age-controlled fossiliferous sites, we quantitatively reconstruct the climates through most of the Paleogene of northeast China and discuss related seasonal variations. Our results demonstrate that the mean annual temperature (MAT) gradient was fairly shallow (0.27 °C/1° latitude) during the Paleocene throughout this region. In the Eocene, seasonality was high in the region, indicated by marked differences in both temperature and precipitation between winters and summers of the sites. The paleo-East Asian monsoon must have had intensified at least in the late mid Eocene, shown by apparent differences in annual precipitation distribution at all the sites. Regarding the Paleogene climatic evolution of northeast China, our quantitative results suggest that MAT overall declined from warm in the Paleocene and Eocene to moderate in the Oligocene, generally consistent with the trend of marine records but with some distinctions. Two significant cooling events are recognized in the early and mid Eocene with MAT 3.4 °C and 3.8 °C lower, and winter temperature 5.8 °C and 4.7 °C lower, respectively, in similar magnitudes to corresponding variations in Europe and North America. Furthermore, the present results show that MAT rebounded in the late mid Eocene and then decreased until the Oligocene, a similar pattern demonstrated in Europe during the mid Eocene to Oligocene interval.

1. Introduction

Paleogene climates are characterized as being in a generally warm and equable "greenhouse" state across the world, punctuated by brief hyperthermals, and a transition to an "icehouse" state by the late Eocene to early Oligocene (Zachos et al., 2008; Eldrett et al., 2009). The climatic evolution during this period provides unique perspectives for the modern global changes that help probe into the integrated response of the Earth system to various driving forces (Zachos et al., 2008; Utescher et al., 2009). Case studies of geological records offer direct evidence to explain the paleoclimatic changes, while model simulations of quantitative paleoclimatic results are of considerable potential for climate prediction, especially for events such as hyperthermals in the latest Paleocene to earliest Eocene interval, the long- and short-lived optima during the Eocene, and the "icehouse" both in the Eocene–Oligocene transition and the latest Oligocene (Sloan and Barron, 1992; Shellito and Sloan, 2006; Zachos et al., 2008; Bijl et al., 2009; Eldrett et al., 2009; Stap et al., 2010; Huber and Caballero, 2011).

The evolution of Paleogene climates has been well studied on the basis of either fossil plants from Australia, Europe and North America (Greenwood and Wing, 1995; Wilf, 2000; Wing and Harrington, 2001; Jolley and Widdowson, 2005; Mosbrugger et al., 2005; Wing et al., 2005; Utescher et al., 2007; Greenwood et al., 2010; Utescher et al., 2011) or marine proxy data from both hemispheres (Pearson et al., 2007; Zachos et al., 2008; Bijl et al., 2009). However, it is only recently that quantitative climatic reconstructions have been conducted on individual sites of the East Asian Paleogene (e.g., He and Tao, 1997; Quan and Zhang, 2005; Su et al., 2009; Hao et al., 2010; Wang et al., 2010). These studies have largely improved the paleoenvironmental interpretations of this vast region, but an overview of the climate trend in East Asia is still lacking. This is mainly because of the poor stratigraphic resolution and confused sampling horizons of plant fossils, limiting paleoclimate simulation at a global scale. For example, Shellito and Sloan (2006) modeled the dynamic progress of vegetation distribution in the early Eocene to examine the vegetation response to coeval climate changes in which studies the East Asian data had to be inferred from North American analogues. On the other hand, Paleogene climatic data have been

* Corresponding authors at: Department of Biological Sciences, 309 Brown Hall, East Tennessee State University. Box 70703, Johnson City, TN 37614-1710, USA. Tel.: +1 423 439 6920; fax: +1 423 439 5958.
E-mail addresses: quan@jlu.edu.cn (C. Quan), liuc@etsu.edu (Y.-S.(C.) Liu).

0031-0182/$ – see front matter
doi:10.1016/j.palaeo.2011.10.016

Fig. 1. Location of plant fossil sites. 1. Wuyun; 2. Fushun; 3. Yilan; 4. Hualin; 5. Shulan; 6. Huanghua; 7. Huadian; 8. Hunchun.

accumulated over recent decades based on both continental quantitative estimates and marine proxy results. It is unfortunate that emphases have been usually imposed on mean annual climatic conditions; as a result, only a few studies have reconstructed the seasonal changes of paleoclimates (e.g., Crowley et al., 1986; Greenwood and Wing, 1995; Eldrett et al., 2009). Seasonal variations play one of the key roles in the climate system that are primarily controlled by land–sea distribution, general atmospheric circulation, and ocean currents (Rohli and Vega, 2008). Therefore seasonality, including annual distributions of both temperature and precipitation, is also critical to paleoclimatic studies.

In this paper, we report the quantitative estimates of Paleogene climate changes throughout northeast China on the basis of independently age-constrained plant fossil assemblages. We focus on the evolution of paleoclimate in this region, particularly the geographical distribution and seasonal variations of the paleoclimates (Fig. 1 and Table 1). Our results demonstrate that the Paleogene climates underwent a generally similar pattern to those revealed by marine isotopic proxies and fossil plants from other continents, but show a strong seasonality indicated by high annual thermal and hydrological differentiations.

2. Selection of plant assemblages, stratigraphical background, and age control

Although dozens of the Paleogene sites have been documented from northeast China (Liu et al., 1996; Zhou and Wu, 2002), a total of 29 plant assemblages from 8 sites were selected in the present study because their ages are well constrained (Fig. 1; Table 2). In general, an assemblage was selected when its age is controlled by at least two independent methods (Table 2). An assemblage whose age is only implied by plant fossils is excluded here, regardless of either its biodiversity and abundance, or its potential importance for paleoclimatic reconstruction of some critical intervals. For example, the flora from Sanhe of Jilin Province has been interpreted as Oligocene based on floristic correlations with the adjacent Korean floras (Guo and Zhang, 2002). This is the only known Oligocene site in northeast China with abundant well-preserved macrofossil plants. However, this flora is precluded from the present study because we lack further corroborative evidence for its age-control.

Among these 8 sites, the fossil assemblages used for analysis of the climate evolution are mainly from the following 3 sites, i.e. Fushun, Shulan, and Yilan, because deposits of these 3 sites span the majority of the Paleogene (Fig. 2; Table 2). Stratigraphically, the Paleogene strata of these 3 sites, whose geological features are briefly summarized below, can be well correlated by geochronological results (Zhao et al., 1994; Huang et al., 1998; Yang et al., 2004; Zhang et al., 2007a, 2007b; Shi et al., 2008a) (Fig. 2). The other 5 sites are mainly used to complement the overall climates in the Paleogene.

The Fushun Opencast Coalmine (Site 2 in Fig. 1) is located in a relatively small east–west-trending exposure of Mesozoic and Cenozoic rocks surrounded by Precambrian terrane (Johnson, 1990; Wu et al., 2002). The strata present in the mine are well exposed along the slopes of excavated pits. These continental sequences consist of swampy to fluvio-deltaic and tuffaceous sediments that were deposited in the basin during the early Paleogene (Hong et al., 1980; Johnson, 1990; Yang and Li, 1997; Wu et al., 2002). In ascending order, the sequence is subdivided into Laohutai, Lizigou, Guchengzi, Jijuntun, Xilutian, and Gengjiajie formations (Fig. 2). This sedimentary sequence across the mid Paleocene to late Eocene lacks noticeable unconformities except for the paraconformity between the first two formations, i.e., the Laohutai and Lizigou formations (Hong et al., 1980; Yang and Li, 1997; Fig. 2). In addition to the paleobotanical record, the ages of these formations have been constrained by evidence of either paleomagnetism, isotopes, or animals (Hong et al., 1980; Zhao et al., 1994; Shi, 2010, personal communication) (Table 2; Fig. 2).

In Shulan of Jilin Province (Site 5 in Fig. 1), the Paleogene sediments with fossil plants are subdivided into 3 units. The Bangchuigou and the overlying Jishu formations span the Eocene period, while the Shuiquliu Formation is aged as the Oligocene (Fig. 2). The Bangchuigou Formation is composed of depositional cyclicity incarnating by the lithological transformations among grey sandy stone, yellow-grey siltstone, green mudstone, and clay, mainly deposited in swampy, lacustrine, and deltaic environments (Li, 1997). The Jishu Formation is further subdivided into the coal-bearing member (the lower member) and upper brown sand- and mudstone member (the upper member) (Fig. 2), deposited alternately in lacustrine, swampy, and fluvial environments (Li, 1997). Paleomagnetic dating results indicate that both the Bangchuigou and Jishu formations span the Eocene Epoch (Zhao et al., 1994). On the other hand, the

Table 1
Modern climate of studied sites. Data are available on the website of China Meteorological Data Sharing Service System (open access to registered user, http://cdc.cma.gov.cn/).

Site	MAT (°C)	CMM (°C)	WMM (°C)	MART (°C)	MAP (mm)	HMP (mm)	LMP (mm)	PWM (mm)	MARP (mm)
1. Wuyun	−1.1	−28.5	20.9	49.4	592	146	5	146	141
2. Fushun	8.1	−11.5	24.5	36.0	684	167	7	167	160
3.Yilan	3.4	−19.5	22.4	41.9	513	138	3	128	135
4. Hualin	3.2	−18.8	22.0	40.8	423	122	4	110	118
5. Shulan	5.2	−16.1	22.6	38.7	576	185	3	185	182
6. Huanghua	3.8	−18.0	21.9	39.9	531	120	4	120	116
7. Huadian	6.2	−14.3	23.4	37.7	634	182	5	182	177
8. Hunchun	5.7	−14.0	21.3	35.3	606	134	5	134	129

Table 2
List of the selected Paleogene sites of northeast China, and sampling stratigraphical units. Site numbers as in Fig. 1. Methods of age control other than pollen assemblage (for detailed literature, refer to the text): B–bird; GD–geochemical dating; L–leaves; M–mammals; PD–Paleomagnetic dating; R–reptiles; SC–stratigraphic correlation. Fossil type: L–leaves; P–pollen.

Site	location	Formation (member)	Age control	Site coordinate	Fossil type	References of fossil flora
Early Paleocene						
1	Wuyun, Heilongjiang	Wuyun (lower)	GD	N49.3°, E129.5°	P	Hao et al., 2010
Mid Paleocene						
1	Wuyun, Heilongjiang	Wuyun (upper)	GD; PD	–	P	Hao et al., 2010
2	Fushun, Liaoning	Laohutai	GD [a]	N41.8°, E123.9°	P	Hong et al., 1980
Late Paleocene						
2	Fushun, Liaoning	Lizigou	GD [a]	–	P	Hong et al., 1980
Early Eocene						
3	Yilan, Heilongjiang	Xin'ancun	GD	N46.1°, E129.3°	P	This study
4	Hualin, Heilongjiang	Bahuli (lower)	PD; SC	N44.8°, E129.8°	P	This study
5	Shulan, Jilin	Bangchuigou	PD	N44.5°, E126.9°	P	Fan, 1985
2	Fushun, Liaoning	Guchengzi	L; PD	–	P; L	Hong et al., 1980
Mid Eocene						
3	Yilan, Heilongjiang	Dalianhe (lower)	GD; L	–	P; L	Liu, 1990; He and Tao, 1997
		Dalianhe (middle)	GD; PD	–	P; L	Liu, 1990; He and Tao, 1997
		Dalianhe (upper)	GD; PD	–	P	Liu, 1990
5	Shulan, Jilin	Jishu (lower)	M; F	–	P	Chen, 1985
		Jishu (upper)	M; PD	–	P	Chen, 1985
6	Mudanjiang, Heilongjiang	Huanghua	GD; L	N44.6°, E129.4°	P; L	This study
7	Huadian, Jilin	Huadian	B; M	N42.9°, E126.7°	P; L	Manchester et al., 2005; this study
8	Hunchun, Jilin	Hunchun (lower)	L; SC	N42.7°, E130.5°	P; L	Liu, 1987
2	Fushun, Liaoning	Jijuntun	PD	–	P; L	Hong et al., 1980; Liu et al., 1996
		Xilutian	PD	–	P	Hong et al., 1980
Late Eocene						
8	Hunchun, Jilin	Hunchun (upper)	L; SC	–	P	Zhang et al., 1987
2	Fushun, Liaoning	Gengjiajie	PD; R	–	P	Qu, 1993
Oligocene						
5	Shulan, Jilin	Shuiquliu	PD	–	P	Chen, 1985; Zhang et al., 2010

[a] Unpublished data by F. Shi (2010, personal communication).

Oligocene Shuiquliu Formation conformably overlies the Jishu Formation in the central basin, but is paraconformable in the margin areas (Li, 1997). It mainly consists of grayish green sandstone, mudstone, and shale, occasionally intercalated with faulty coal seam (Li, 1997).

At the Yilan site in Heilongjiang Province (Site 3 in Fig. 1), the Xin'ancun and the overlying Dalianhe formations, which span the Eocene (Fig. 2), have mainly developed in the north Fangzheng faulted depression (Shi et al., 2008a). Their ages are mainly controlled by the fission track dating result (54.9 ± 0.5 Ma for the bottom of Xin'ancun Formation, and 37.4 ± 0.3 Ma for the top of Dalianhe Formation, respectively) (Huang et al., 1998; Yang et al., 2004; Zhang et al., 2007a; Shi et al., 2008a; Shi, 2011, personal communiucation). The facies are composed mainly of fluvial, slough, and lacustrine, lithologically including coal, glutenites, oil shale, sandy shale, and sandstone. From bottom to top, the Dalianhe Formation is further subdivided into three conformable members (Fig. 2), i.e., the lower coal-bearing member, the middle oil shale member, and the upper sandstone member (Liu, 1990).

It should be mentioned that Hao et al. (2010) reconstructed the Paleocene environments of Jiayin area based on palynological data from the Wuyun Formation. This study is of importance because it is the first Coexistence Approach (CA) study for understanding the climate evolution of NE Chinese Paleogene. However, both this and a previous study (Quan and Zhang, 2005) fail to provide the accurate age constraints on the Wuyun Coalmine section (i.e., the upper member of the Wuyun Formation; Fig. 2), which was mistakenly attributed to the late early Paleocene (late Danian). As shown by Zhao et al. (1994), the magnetostratigraphical study suggested that the deposition of the Wuyun Coalmine section occurred during the polarity chron C27–C26, indicative of a mid Paleocene age. Furthermore, Sun et al. (2005) reported that the $^{40}Ar/^{39}Ar$ dating on the tuff layer of the Baishantou section (i.e., the lower member of Wuyun Formation; Fig. 2) a 61.0 ± 2.5 Ma, corroborated by the zircon fission track dating age of 61.9 ± 1.3 Ma (Shi et al., 2008a). Thus, it should be safe to conclude that the age of Wuyun Coalmine section can not be earlier than Selandian (mid Paleocene) (Fig. 2). Consequently, the Wuyun Coalmine section in north Heilongjiang Province can be correlated with the Laohutai Formation of Fushun, Liaoning Province (Figs. 1 and 2).

3. Methods

In recent decades the quantitative methodologies for paleoclimate reconstructions using fossil plants have made great strides. Two main approaches have been developed and are widely used for quantitative estimation of paleoclimatic parameters, e.g., the Coexistence Approach (CA) (Mosbrugger and Utescher, 1997) and leaf physiognomical analyses (Wing and Greenwood, 1993; Wolfe, 1993; Greenwood et al., 2004; Su et al., 2010; Peppe et al., 2011; Spicer et al., 2011). In the present study, because the majority Chinese records are microfossils, the CA is applied. This approach is organ-independent, so that both macro- and microfossil plants are eligible as long as their modern affinities are determinable (Mosbrugger and Utescher, 1997; Utescher et al., 2007; Bruch et al., 2011). The CA uses the climate tolerances of all nearest living relatives (NLRs) known for a given fossil flora by assuming that the tolerances of a fossil plant are not significantly different from its modern counterpart (Mosbrugger and Utescher, 1997; Utescher et al., 2007). Using the taxa-climate database compiled by Utescher and Mosbrugger (1997–2011), "coexistence intervals" of climatic parameters can be calculated, which are considered as the best comparable environmental conditions of the given fossil location.

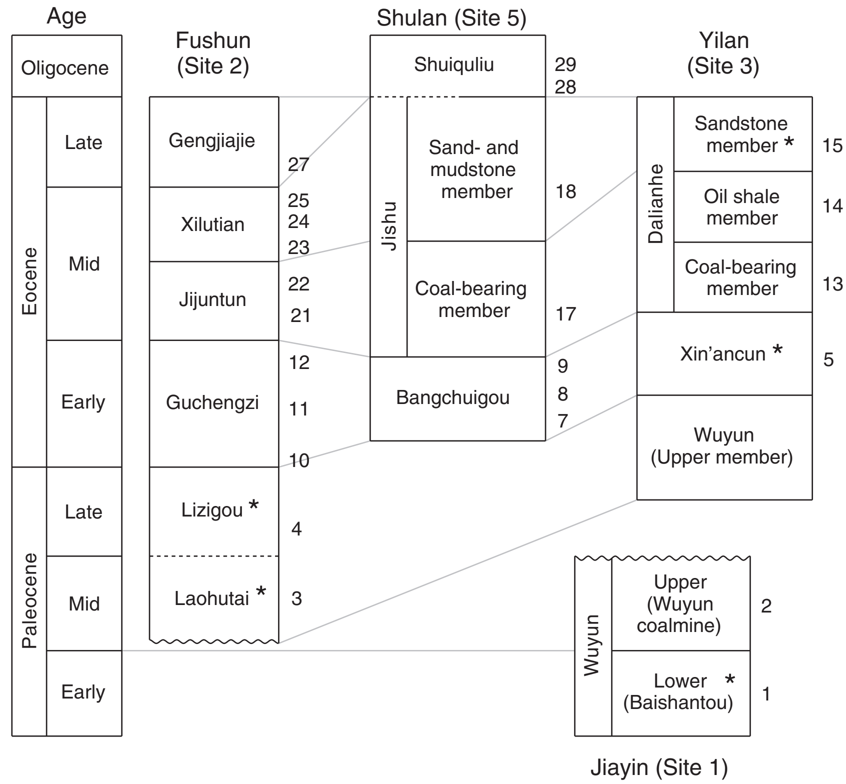

Fig. 2. Stratigraphical correlation among 4 main sites. Numbers right to each unit represent the approximate sampling horizon of particular plant assemblage. Asterisk indicates formation with isotopic dating: lower parts of both the Laohutai and Lizigou formations of Fushun—61.0 ± 0.4 Ma and 58.0 ± 0.3 Ma, respectively (zircon fission track dating; Shi, 2010, personal communication); upper part of the Baishantou member of the Wuyun Formation, Jiayin—61.0 ± 2.5 Ma ($^{40}Ar/^{39}Ar$ dating; Sun et al., 2005) and 61.9 ± 1.3 Ma (fission track dating; Shi et al., 2008a); bottom of the Xin'ancun Formation and top of the Dalianhe Formation, Yilan—54.9 ± 0.5 Ma and 37.4 ± 0.3 Ma, respectively (fission track dating; Huang et al., 1998; Yang et al., 2004; Zhang et al., 2007a).

The fossil plant data analyzed here include both compilations from the literature and our collections. The determination of NLRs of fossil groups is designated only to the generic level, and sometimes to the family level (Appendix A), due to the facts that we can not exactly link a fossil species to a certain modern taxonomical affinity as discussed by Liu et al. (2011). For NLR determinations of fossil pollen and spores, we follow Song et al. (1999), who comprehensively reviewed the Late Cretaceous to Neogene palynological records and the pollen sequence correlations in the Cenozoic palynofloristic regions throughout China. The paleoclimatic reconstructions are queried from the Palaeoflora Database. For taxa unavailable in the database, we follow the procedures stated in Liu et al. (2011). Several fossil taxa are excluded in the reconstruction process because they contribute little to determining climatic tolerances (e.g., extinct, cosmopolitan, and aquatic taxa), or because their NLRs no longer occupy the range of climatic conditions they can tolerate, i.e. relicts such as *Ginkgo* and *Metasequoia*.

Facilitated by the program ClimStat, 7 climatic parameters are reconstructed, i.e. mean annual temperature (MAT, °C), mean temperature of the warmest month (WMM, °C), mean temperature of the coldest month (CMM, °C), mean annual precipitation (MAP, mm), mean precipitation of the warmest month (WMP, mm), mean precipitation of the driest month (LMP, mm), and mean precipitation of the wettest month (HMP, mm). In addition, 2 parameters, the mean annual range of temperature (MART—the temperature difference between of warmest and coldest months, °C) and the mean annual range of precipitation (MARP—the difference between wettest and driest months, mm), are further calculated by differences of mean values between the WMT and CMT, and HMP and LMP, respectively. These parameters provide detailed information on both geographic climate pattern of particular age and the climate evolution in the Paleogene.

4. Results

Intervals of a total of 7 climatic parameters are directly calculated by the CA as shown in Table 3. The mean values of coexistence intervals along with the other 2 parameters (MART and MARP) are calculated for a direct comparison regarding the climates throughout the region over time (Table 4).

In general, most of the estimated temperature parameters, especially MATs, are of inherent consistency represented by errors less than 2.0 °C (for more than half of them, <1.0 °C), with an error range of 1–15% to the mean value (Table 4). The MAP results, however, have relatively large error ranges, varying about 2–53% to the mean value (Table 4). But given the error ranges, the results still show a detectable climatic differentiation in the NE Chinese Paleogene.

4.1. Temperatures

The NE Chinese early Paleocene climates are only represented by a flora from the lower Wuyun Formation of Jiayin, Heilongjiang Province. The CA results by Hao et al. (2010) indicate that it had an MAT of 14.8–16.6 °C and an MAP of 816–1389 mm (Table 3). The mid Paleocene climates are largely defined by the assemblage from the upper Wuyun Formation of Jiayin, Heilongjiang Province in the north (Site 1, Assemblage 2) and that from the Laohutai Formation of Fushun, Liaoning Province in the south (Site 2, Assemblage 3) (Figs. 1 and 2; Table 3). Although the MATs and WMTs of both sites are similar, the CMT of Laohutai (9.6–12.5 °C, with a mean value of 11.1 °C) is significantly higher than that of both the upper and lower Wuyun (3.6 °C).

The early Eocene climates are reconstructed on the basis of 8 assemblages from 4 sites (Table 3; Fig. 1). Except for the unexpected low MAT of the early Guchengzi stage in Fushun (Site 2, Assemblage

Table 3
Quantitative reconstruction of climate parameters for all the 29 plant assemblages (PA) from 8 sites of NE China (arranged by geological age; site number as in Fig. 1 and Table 2).

Site	PA	Formation (sampling horizon/member)	MAT(°C)	CMM (°C)	WMM (°C)	MAP(mm)	HMP (mm)	LMP (mm)	PWM (mm)
Early Paleocene									
1	1[a]	Wuyun (lower)	14.8–16.6	3.6	22.5–283.	815–1389	183–245	10–24	–
Mid Paleocene									
1	2[a]	Wuyun (upper)	14.8–16.6	3.6	23.9–28.3	1202–1389	198–245	10–24	–
2	3	Laohutai	16.5–18.4	9.6–12.5	24.7–26.8	897–1355	109–153	24–41	84–142
Late Paleocene									
2	4	Lizigou	17.9–18.3	7.0–10.2	24.7–26.8	897–1355	109–153	24–37	84–142
Early Eocene									
3	5	Xin'ancun	17.9–18.4	7.0–12.5	27.3–27.9	1035–1355	187–195	18–41	93–154
4	6	Bahuli (lower)	13.6–18.4	3.7–12.5	23.6–28.1	961–1577	109–241	16–41	99–175
5	7	Bangchuigou (lower)	15.2–18.4	7.0–7.8	24.0–25.6	1035–1355	134–195	18–41	139–141
	8	Bangchuigou (middle)	17.9–18.4	7.0–12.5	24.0–27.9	1304–1355	148–196	16–41	139–141
	9	Bangchuigou (upper)	15.7–16.1	6.6–7.0	24.7–25.6	1122–1206	134–143	25–41	115–142
2	10	Guchengzi (lower)	13.3–16.1	1.7–7.0	20.0–25.6	373–1206	130–143	25–45	45–61
	11	Guchengzi (middle)	15.2–15.6	1.7–7.8	23.0–25.6	1035–1362	134–143	25–45	93–142
	12	Guchengzi (upper)	17.9–21.1	7.0–13.3	28.1–28.3	897–1355	109–196	50–64	84–154
Mid Eocene									
3	13	Dalianhe (lower)	20.6–20.8	3.7–4.4	26.5–26.8	1122–1362	116–153	24–43	108–111
	14	Dalianhe (middle)	13.3–15.6	2.2–4.4	25.0–26.8	979–1281	116–153	18–24	108–111
	15	Dalianhe (upper)	15.7–18.4	5.0–12.5	24.7–27.9	1304–1355	148–195	18–37	139–154
6	16	Huanghua	17.9–18.3	7.0–10.2	24.7–27.7	1122–1355	115–195	19–38	84–154
5	17	Jishu (coal)	15.6–18.4	7.0–7.8	24.7–25.0	897–1206	109–143	18–41	84–143
	18	Jishu (sandstone)	15.6–18.4	7.0–7.8	24.7–25.0	897–1206	109–143	18–67	84–141
7	19	Huadian	15.6–18.4	3.8–12.5	24.7–27.9	1194–1355	116–195	21–24	118–154
8	20	Hunchun (lower)	16.5–18.4	6.6–7.8	27.3–27.9	1096–1206	187–195	18–24	139–141
2	21	Jijuntun (lower)	16.5–18.3	7.4–8.1	26.0–26.8	1122–1215	148–153	19–24	120–142
	22	Jijuntun (upper)	11.6–15.6	1.7–4.4	23.0–26.8	735–1362	109–153	24–41	49–61
	23	Xilutian (lower)	15.2–15.6	3.7–4.4	23.6–26.8	1035–1362	134–153	24–41	99–142
	24	Xilutian (middle)	16.5–21.1	5.5–13.3	24.7–26.8	897–1355	109–153	24–45	99–142
	25	Xilutian (upper)	15.2–21.1	6.6–13.3	24.0–28.1	1035–1355	134–196	12–45	93–154
Late Eocene									
8	26	Hunchun (upper)	17.9–18.4	7.0–12.5	27.3–28.1	1096–1520	216–236	14–24	173–175
2	27	Gengjiajie	17.9–18.4	7.0–12.5	27.3–28.1	897–1355	187–195	18–24	99–154
Oligocene									
5	28	Shuiquliu (lower)	15.6–16.1	5.0–7.8	24.7–25.6	823–1206	109–143	21–41	79–141
	29	Shuiquliu (upper)	11.6–16.1	−0.1–7.8	22.8–25.6	578–1206	102–143	9–41	45–143

[a] Data from Hao et al. (2010).

10), all the others show a high MAT (>15 °C) and moderate CMT (≥4.8 °C) (mean value; Tables 3 and 4). The mid Eocene climates are reconstructed on the basis of 13 assemblages from 6 sites, which demonstrate a relatively high differentiation (Table 3; Fig. 1). The highest MAT is detected from the lower Dalianhe Formation (20.7 °C) of Heilongjiang Province (Site 3, Assemblage 13), while the lowest MAT is found in the upper Jijuntun Formation (13.6 °C; Site 2, Assemblage 22) (Tables 3 and 4). All the other assemblages indicate that temperatures of each site were relatively high during the specific episodes, with MATs > 15 °C and CMTs > 4 °C (Table 4).

The Oligocene climates are estimated based on 2 assemblages from the Shuiquliu Formation of Jilin Province. The results show an overall cooling from the late Eocene to the Oligocene (Table 3).

4.2. Precipitation

The quantitative results from all the plant assemblages are given in Table 3, while their mean values and error bars are shown in Table 4. Except for the assemblage 10 of Liaoning Province (early Guchengzi stage) and Assemblage 29 of Jilin (late Shuiquliu stage), all the other assemblages yield results of mean annual precipitation exceeding 1000 mm during the Paleogene. However, seasonal variability in precipitation appears to occur in most sites. The wet summers with high precipitation occurred in most sites (WMPs > 110 mm; Tables 3 and 4), whereas the winters were fairly dry with quite low precipitation (LMPs < 35 mm; Tables 3 and 4).

It should be pointed out that the climatic parameters derived from these assemblages are not always subjected to direct comparisons from one site to the other, largely due to the different stratigraphical and chronological resolutions of each site and, in consequence, the different age of specific assemblage therefrom. Therefore the discussion of the Paleogene climate evolution of northeast China will be addressed mainly in a vertical comparison at each site, although a rough horizontal comparison among the sites will be considered.

5. Discussion

5.1. Mid Paleocene temperature gradients

The two sites, Wuyun in the north and Fushun in the south, provide an excellent example to discuss the mid Paleocene meridional temperature gradients of northeast China (Fig. 1). The reconstructed MAT of Fushun is 16.5 °C–18.4 °C with a mean value of 17.5 °C (Tables 3 and 4), while the MAT of Wuyun is 14.8 °C–16.6 °C with a mean value of 15.7 °C (Hao et al., 2010). The difference in paleolatitude of the two sites is about 6.6° (38.1°N for Fushun, and 44.7°N for Wuyun, respectively; Zhao et al., 1994). These results deduce a

Table 4
Mean values and their error bars of climate parameters reconstructed by the CA, and inferred MART and MARP of the selected Paleogene plant assemblages (PA) from NE China (arranged by geological age; site and PA numbers as in Fig. 1 and Tables 2 and 3).

Site	PA	MAT (°C)		CMT (°C)		WMT (°C)		MAP (mm)		HMP (mm)		LMP (mm)		WMP (mm)		MART (°C)	MARP (mm)
		Mean	Bar	Mean	Bar	Mean	Bar	Mean	Bar	Mean	Bar	Mean	Bar	Mean	Bar		
Early Paleocene																	
1	1 [a]	15.7	0.9	3.6	0.0	25.4	2.9	1103	287	215	31	17	7	–	–	21.8	198
Mid Paleocene																	
1	2 [a]	15.7	0.9	3.6	0.0	26.1	2.2	1296	94	222	7	17	7	–	–	22.5	205
2	3	17.5	0.9	11.1	1.5	25.8	1.1	1126	229	131	22	33	9	113	29	14.7	99
Late Paleocene																	
2	4	18.1	0.2	8.6	1.6	25.8	1.1	1126	229	131	22	31	7	113	29	17.2	101
Early Eocene																	
3	5	18.2	0.3	9.8	2.8	27.6	0.3	1195	160	191	4	30	12	124	31	17.9	162
4	6	16.0	2.4	8.1	4.4	25.9	2.3	1269	308	175	66	29	13	137	38	17.8	147
5	7	16.8	1.6	7.4	0.4	24.8	0.8	1195	160	165	31	30	12	140	1	17.4	135
	8	18.2	0.3	9.8	2.8	26.0	2.0	1330	26	172	24	29	13	140	1	16.2	144
	9	15.9	0.2	6.8	0.2	25.2	0.5	1164	42	139	5	33	8	129	14	18.4	106
2	10	14.7	1.4	4.4	2.7	22.8	2.8	790	417	137	7	35	10	53	8	18.5	102
	11	15.4	0.2	4.8	3.1	24.3	1.3	1199	164	139	5	35	10	118	25	19.6	104
	12	19.5	1.6	10.2	3.2	28.2	0.1	1126	229	153	44	57	7	119	35	18.1	96
Mid Eocene																	
3	13	20.7	0.1	4.1	0.4	26.7	0.2	1242	120	135	19	34	10	110	2	22.6	101
	14	14.5	1.2	3.3	1.1	25.9	0.9	1130	151	135	19	21	3	110	2	22.6	114
	15	17.1	1.4	8.8	3.8	26.3	1.6	1330	26	172	24	28	10	147	8	17.6	144
6	16	18.1	0.2	8.6	1.6	26.2	1.5	1239	117	155	40	29	10	119	35	17.6	127
5	17	17.0	1.4	7.4	0.4	24.9	0.2	1052	155	126	17	30	12	114	30	17.5	97
	18	17.0	1.4	7.4	0.4	24.9	0.2	1052	155	126	17	43	25	113	29	17.5	84
7	19	17.0	1.4	8.2	4.4	26.3	1.6	1275	81	156	40	23	2	136	18	18.2	133
8	20	17.5	0.9	7.2	0.6	27.6	0.3	1151	55	191	4	21	3	140	1	20.4	170
2	21	17.4	0.9	7.8	0.4	26.4	0.4	1169	47	151	3	22	3	131	11	18.7	129
	22	13.6	2.0	3.1	1.4	24.9	1.9	1049	314	131	22	33	9	55	6	21.9	99
	23	15.4	0.2	4.1	0.4	25.2	1.6	1199	164	144	10	33	9	121	22	21.2	111
	24	18.8	2.3	9.4	3.9	25.8	1.1	1126	229	131	22	35	11	121	22	16.4	97
	25	18.2	3.0	10.0	3.4	26.1	2.1	1195	160	165	31	29	17	124	31	16.1	137
Late Eocene																	
8	26	18.2	0.3	9.8	2.8	27.7	0.4	1308	212	226	10	19	5	174	1	18.0	207
2	27	18.2	0.3	9.8	2.8	27.7	0.4	1126	229	191	4	21	3	127	28	18.0	170
Oligocene																	
5	28	15.9	0.3	6.4	1.4	25.2	0.5	1015	192	126	17	30	12	110	31	18.8	97
	29	13.9	2.3	3.9	4.0	24.2	1.4	892	314	123	21	21	16	94	49	20.4	98

[a] Data from Hao et al. (2010).

flat MAT gradient of about 0.27 °C/1° latitude, compared to a modern gradient of about 0.82 °C/1° latitude in this area.

The Paleocene MAT gradient derived from marine data is about 0.28 °C/1° latitude in the Northern Hemisphere (Tripati et al., 2001), which is close to the result of the present study. Davies-Vollum (1997) obtained a Paleocene gradient of 0.3 °C/1° latitude based on macrofossil plants from the western interior of North America, slightly stronger than the Chinese result. As seen in the modern world, the latitudinal gradients of temperature more or less vary on different continents and/or different scales, because of specific geographical features such as ocean-continent configuration, topography, and/or ocean currents (e.g., Greenwood and Wing, 1995; Tripati et al., 2001; Roberts et al., 2009). Therefore, despite some degree of variation, all the available Paleocene data are comparable, showing a low meridional difference in MAT. This also indicates that the Paleocene MATs in upper mid latitudes were remarkably more equable in distribution than those of today.

It is interesting that CMTs of the two sites appear greatly different, although both of their MATs and WMTs are very close (Tables 3 and 4). With shallow gradients of MAT and WMT in this region as indicated above, the CMT of Jiayin area (3.6 °C) is considerably lower than that of Fushun (11.1 °C), suggesting that the Jiayin area underwent a highly stronger thermal seasonality in the mid Paleocene (Table 4). Meanwhile, the reconstructed winter temperatures in Fushun and Jiayin generate a CMT gradient of about 1.13 °C/1° latitude. However, this steep CMT gradient may generate freezing Arctic winters, potentially inconsistent with some generally accepted Paleocene global climate reconstructions. For example, the Paleocene climate is believed to have experienced "greenhouse" conditions, having an ice-free North polar region, and without winter freezing in the Arctic Ocean (Bice et al., 1996; Zachos et al., 2008). But the 1.13 °C/1° latitude CMT gradient would yield a freezing winter in a region just about 3° latitude or more north of Jiayin. Furthermore, a study on mollusc stable isotopes from the Arctic Ocean demonstrates that there was a very moderate seasonality in high-latitude marine temperatures during the Paleocene, with a mean annual shallow-marine temperature of about 11 °C and MART of about 6 °C (Bice et al., 1996). This MART is far less than that of Jiayin (22.5 °C; Table 4). Therefore, even though it could be assumed as a case of a special regional continental climate pattern partially because the landmass tends to experience more thermal variation than the ocean by its lower specific heat capacity, as clearly seen in the modern world (Sloan and Barron, 1992; Rohli and Vega, 2008), more detailed and extensive Paleocene CMT data from other mid-high latitude areas or from a larger geographical scale are needed to further explain this gradient phenomenon.

5.2. Eocene seasonality

The Eocene is one of the most characterized epochs of "greenhouse" climate in geological history, marked by distinguishable global warming, and thereby an equable meridional distribution of temperatures (Sloan and Barron, 1992; Greenwood and Wing, 1995; Bijl et al., 2009). However, few data are available so far detailing seasonal climatic variations represented by CMT and WMT (e.g., Wing and Greenwood, 1993; Eldrett et al., 2009). These two climatic parameters are critical to determine the mean annual range of temperature (MART), and hence partly the continentality.

All the estimated NE Chinese Eocene climates are subtropical (sensu Wolfe, 1993), with MATs higher than 13 °C and MAPs no less than 790 mm (mean value; Table 4; Fig. 3A). Seasonality is evident to a certain degree for the entire Eocene, demonstrated by differentiation of both temperatures and precipitation in summers and winters (Table 4, Fig. 3A–D). Furthermore, the early Eocene assemblages are grouped into two clusters by moderate MARTs but high MARPs of Heilongjiang and Jilin provinces in the north and both moderate MARTs and MARPs of Liaoning Province in the south, consistent with the latitudinal temperature gradients (Fig. 3E). Due to the different stratigraphic resolutions of the mid Eocene sites, MART-MARP clusters appear not to provide a detectable pattern of continentality (Fig. 3F).

The reconstructed climates indicate that different driving forces might have been associated with summer and winter paleoclimates in northeast China. A more or less equable summer temperature throughout the Eocene is indicated by less varied WMTs over all

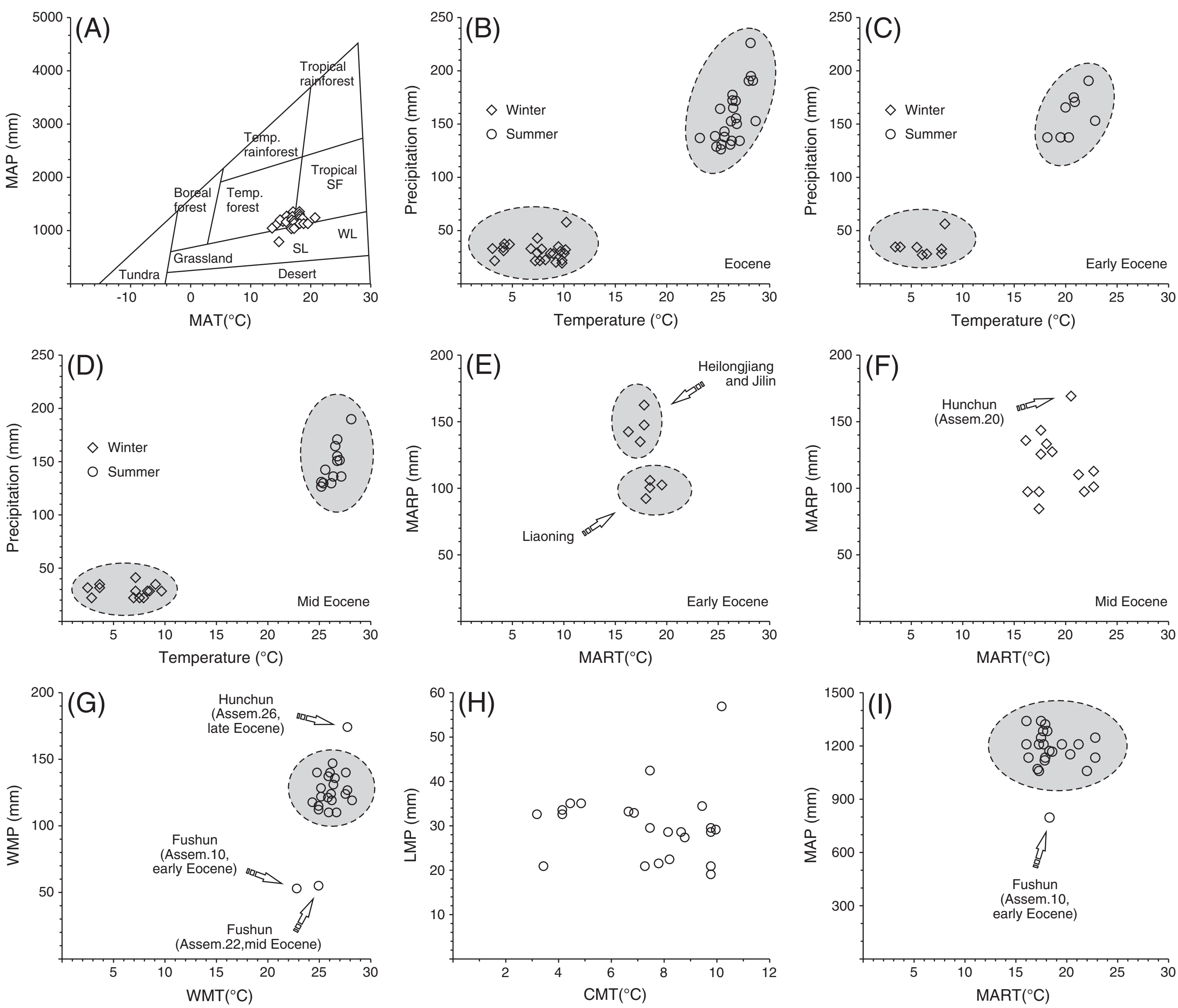

Fig. 3. Eocene climatic characteristics illustrated by plotting a different combination of climatic variables. A–Climatic distribution of studied plant assemblages; biomes follow Whittaker (1975); SF, seasonal forest; SL, shrubland; WL, woodland; B–seasonality in all Eocene plant assemblages represented by high annual differentiations in both temperature and precipitation; C–early Eocene seasonality; D–mid Eocene seasonality; E–relationship between the early Eocene MARTs and MARPs, showing two clusters of Heilongjiang and Jilin provinces in the north and Liaoning Province in the south; F–equable but random distribution of the mid Eocene climate; G–highly correlated WMTs and WMPs showing uniform forcing of summer climate with exception of the late Eocene Hunchun and two "cooling" episodes in mid and early Eocene Fushun; H–evenly distributed winter climate that might be caused by the different age resolutions; I–homogenous continentality of northeast China in the Eocene, with an isolated early Eocene Fushun (Assemblage 10) indicative of a cooling event. The data for plotting are from Table 4, but they are rearranged in geographical and geological order in Appendix B for an easy reading.

sites (Table 4). Along with the high corresponding WMPs (Tables 3 and 4; Fig. 3G), it suggests that this region would have been under equable summer climates, contributed, most probably, from warm and humid airflows from the seas (Fig. 1). Especially, as shown in Fig. 3F and G, the Hunchun area might have experienced wetter summers during the mid-late Eocene. The coastal location of Hunchun might have accounted for the higher WMP, while a significant enhancement of paleo-East Asian monsoon system may have also contributed to hot and humid summers but relatively dry winters (e.g., Huber and Goldner, 2011; Quan et al., 2011).

The cold month climates, however, seem to be greatly complicated. Unlike those of the summer climates, no detectable interrelationship has been observed between the temperature (CMT) and precipitation (LMP) (Fig. 3H), probably because of the uplifted elevation in the west of this region (e.g., the Da Hinggan Mts; Shao et al., 2005), which could alter the winter monsoon (Quan et al., 2011). In addition, an apparent homogeneity of continentality is exhibited, defined by MARTs and corresponding MAPs (Fig. 3I), with the exception of a cooling episode in the early Eocene of Fushun (Assemblage 10 of Site 2; Fig. 3I). Moreover, most of the sites are observed to have low LMPs (Table 4), which suggests that the Eocene winter climates in northeast China were fairly dry, probably resulting from seasonal wind shifts controlled by the paleo-East Asian winter monsoon (Quan et al., 2011).

5.3. Paleoclimates of Fushun

Because the Fushun strata span the majority of the Paleogene (Fig. 2), we here compare the paleoclimatic data of Fushun to those of both terrestrial and marine records from other regions to detail the continental climates of northeast China (Fig. 4). The estimated continental climates of Fushun during the mid Paleocene–late Eocene are characterized by pronounced fluctuations in temperature. The temperature parameters, including MAT, WMT, and CMT, show an oscillating pattern throughout the Eocene consistent with that derived from the marine isotope data (Fig. 4), which have not been recognized in previous studies (Shi et al., 2008b; Su et al., 2009; Wang et al., 2010). With MAT ranging from 11.6 °C to 21.1 °C, WMT from 20.0 °C to 28.3 °C, CMT from 1.7 °C to 13.3 °C, and MAP from 735 mm to 1362 mm (Tables 3 and 4; Fig. 4), subtropical climate conditions are indicated (sensu Wolfe, 1993). However, despite the high MAP, low precipitation in dry months (LMP) is estimated from almost all the plant assemblages, suggesting the development of the monsoonal climate (Tables 3 and 4).

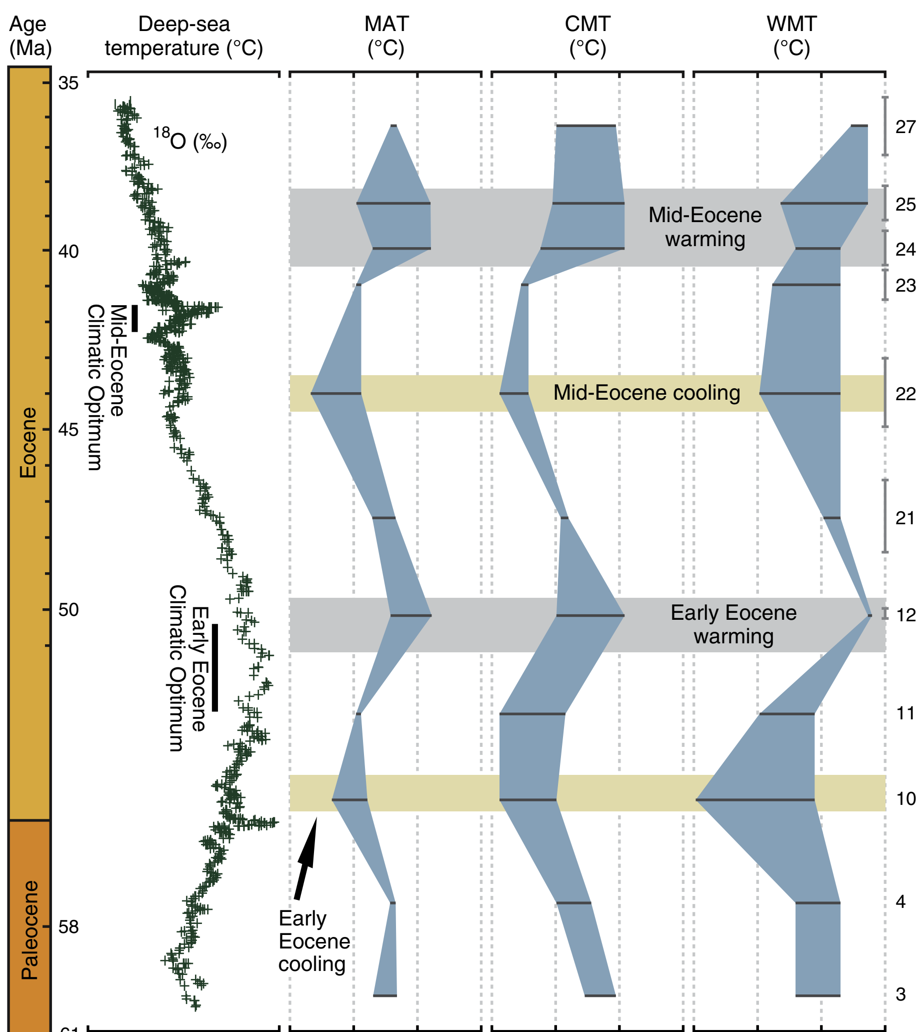

Fig. 4. Temperature evolution of the Early Paleogene Fushun in comparison with the marine oxygen isotope record. The marine data ($\delta^{18}O$) are from Zachos et al. (2008). The horizontal bars represent coexistence intervals of each climatic parameter of Fushun. Code numbers marked along the WMT curve represent individual assemblage from respective formation as shown in Tables 3 and 4. Vertical bars right to the assemblages 12, 21–25, 27 represent the estimated age error range of respective assemblage according to the strata thickness of each assemblage based on the paleomagnetic results of Zhao et al. (1994).

It is clear that two prominent "greenhouse" episodes are observed in early and mid Eocene times, geochronologically corresponding to the Early Eocene Climatic Optimum (EECO) and Mid-Eocene Climatic Optimum (MECO), respectively (Fig. 4). During the EECO, the Fushun temperatures rose from 13.3–16.1 °C to 17.9–21.1 °C in the early to mid Eocene, with a mean increase of 4.8 °C (Tables 3 and 4; Fig. 4). Due to the inherent relatively low resolution of terrestrial strata, currently it appears not possible for us to pinpoint the whole duration of the EECO in northeast China; but the warming trend prevails in all the three geographically separate localities, indicating the EECO exerted equable influence over northeast China (Tables 3 and 4). Both marine isotopic records and North American terrestrial data suggest that this long-term global warming lasted for at least 2 Ma, resulted in the expansion of warm temperate-subtropical biota into high and ice-free polar latitudes (Greenwood and Wing, 1995; Zachos et al., 2008; Woodburne et al., 2009; Greenwood et al., 2010).

The MECO is recognized from the Xilutian Formation of Fushun, in which the MAT rose from 15.2–15.6 °C in the early stage to 16.5–21.1 °C in the middle then 15.2–21.1 °C in the late, with a mean increase of 3.4 °C (Tables 3 and 4; Fig. 4). The MECO is identified as a transient event that lasted less than 0.5 Ma (Fig. 4). However, in northeast China, although having a similar temperature variation pattern and warming magnitude, the terrestrial MECO appears to lag behind that of the marine isotopic results, and be sustained for a much longer time (Fig. 4). This is probably because of different stratigraphic resolutions between the marine and terrestrial data, or the lag may represent a different thermal event that has not previously been recognized.

Although the early Paleogene warming trends have been well documented, mainly from marine deposits (Zachos et al., 2008), a notable continental cooling period has been reported from the Bighorn Basin, Wyoming, based on the oxygen isotope and fossil plants (Wing et al., 2000). The isotopic data suggest that the temperature dropped 3.5–4.0 °C during the short period of ~0.7 Ma after the Paleocene–Eocene thermal maximum (PETM), while the leaf margin analysis suggests that the temperature declined from 18.2 °C to 10.8 °C, followed by a rapid rebound to 15.8 °C then 22.2 °C (Wing et al., 2000). A similar cooling event has been documented by palynological assemblages from the North Sea Basin of northwest Europe, inferring a temperature decrease in the range of 3.0–5.0 °C by the assemblage shift from a humid warm temperate angiosperm forest to a drier mixed mesophytic forest in the Balder Formation interval (Jolley and Widdowson, 2005). Interestingly, our data from northeast China show a similar cooling pattern in the early Eocene, resulted from a MAT shift from 18.1 °C in the Lizigou stage to 14.7 °C in the earliest Guchengzi stage (Table 4; Fig. 4). At this stratigraphic level, even though we at present lack either absolute chronological data or diagnostic Eocene marker taxa as in North America, such as the aquatic fern *Salvinia preauriculata* and the weedy tree *Platycarya* spp. (Wing et al., 2000), pollen assemblage of the earliest Guchengzi stage strongly indicates an early Eocene age (Hong et al., 1980). This assemblage is characterized by the dominance of *Momipites*, *Alnipollenites* and *Pistillipollenites*, and the first appearance of *Tiliaepollenites*, *Ludwigia trilobapollenites*, and *Tricolporopollenites hoshyamaensis*, and distinguishes it from those of the conformably underlain Lizigou Formation (Hong et al., 1980). In other words, the lowermost layer of the Guchengzi Formation was most likely deposited immediately after the Paleocene–Eocene transition (Assemblage 10 in Figs. 2 and 4).

The mean amplitude of the MAT decline during the early Eocene in northeast China is about 3.4 °C (Assemblage 10 in Table 4 and Fig. 2), quite consistent with those of the palynological inference from west Europe (Jolley and Widdowson, 2005) and the isotopic result from North America (Wing et al., 2000). The foliar physiognomic result from North America on the cooling event is nearly double that of the others (7.4 °C), probably resulting from different parts of short-term climatic cycles (Wing et al., 2000) and/or taphonomical biases. Even though the magnitude varies in individual studies, these largely compatible results from different areas illustrate that continents of the North Hemisphere underwent a remarkable cooling period during the earliest part of the Eocene. Geochronologically, this cooling event observed on continents might coincide with the dramatic temperature decline immediately after the PETM shown by marine isotope analyses, which is also of a similar magnitude, dropping from about 12.9 °C on the crest to 9.7 °C in the trough (Table 4; Fig. 4). Jolley and Widdowson (2005) suggested that frequent repletion of coeval volcanic eruptions along the North Atlantic Rift might be responsible to this cooling event; but this mechanism is subject to further corroboration.

Another notable cooling event and subsequent warming event occurred in the mid Eocene (Fig. 4). However, unlike the early Eocene cooling in which both CMT and WMT were significantly dropped (Table 4; Fig. 4), the mid Eocene cooling of 3.8 °C in MATs, while the coeval WMTs remained relatively stable, mainly resulted from the change of CMTs that decreased from 7.8 °C to 3.1 °C with a magnitude of 4.7 °C, (Table 4; Fig. 4). Therefore, it appears that the thermal source in summers was comparatively steady, while cold air currents intensified in the mid Eocene winters (Fig. 4).

It should be mentioned that the preliminary CA results of the mid Paleocene to Eocene climates of Fushun, Liaoning Province reported by Wang et al. (2010), are based upon the same floral dataset of Site 2 as the present study. However, the results of these two studies significantly differ from each other not only in exact parameter values, but also in the general trend of climate evolution during this interval. Our results demonstrate a visible fluctuation in MAT with a maximum magnitude of about 5.8 °C (Table 3; Fig. 4). This fluctuation pattern is largely corroborated by the results from the other two sites in Jilin and Heilongjiang provinces (Table 4; figure not shown), which all match well with marine records (Fig. 4). On the contrary, only a maximum magnitude of 1.9 °C was obtained by Wang et al. (2010). Moreover, two remarkable cooling and two subsequent warming processes are shown in our Fushun results (Fig. 4), while only one slight warming episode with a magnitude of about 1.8 °C was observed in Wang et al. (2010). Several factors might have caused these differences. For example, different NLR selecting strategies are used in these two studies. Many of NLRs are determined to a species level by Wang et al. (2010), while only to a genus or even family level in the present study as already addressed above (Appendix A). Furthermore, these 2 studies have different time resolutions. Wang et al. (2010) treated each formation as a whole (5 in total), while the paleobotanical data from 11 stratigraphical horizons are used in the present study. However, given the differences that exist in these 2 independent studies, they both show a subtropical climate (MAT) in the early Paleogene Fushun area.

5.4. Paleogene temperature evolution

In the present study, only one early Paleocene assemblage from Jiayin of Heilongjiang Province (Site 1 in Figs. 1 and 2) and two Oligocene assemblages from Shulan of Jilin Province (Site 5 in Fig. 1) meet our criteria of floral selection, but the two sites fail to preserve complete spectra of Paleogene floral data (Table 3). The Fushun site, however, yields a flora spanning the majority of the Paleogene (Site 2 in Figs. 1 and 2), although the strata of the lower Paleocene and Oligocene are missing (Fig. 2). To get an overview of the temperature evolution in northeast China throughout the Paleogene, we use the available quantitative data reconstructed from Fushun, i.e., the mid Paleocene to late Eocene (Fig. 2), supplemented by data from the early Paleocene of Jiayin and the Oligocene of Shulan, which can be readily converted through paleotemperature gradients. The three gradients of Paleocene temperatures (MAT, CMT, and WMT), as recognized above, are used to deduce the temperature condition of Fushun. The converted early Paleocene MAT, CMT, and WMT in the Fushun area are about 17.5 °C, 5.4 °C, and 27.2 °C, respectively (Fig. 5). On the other hand, because the general

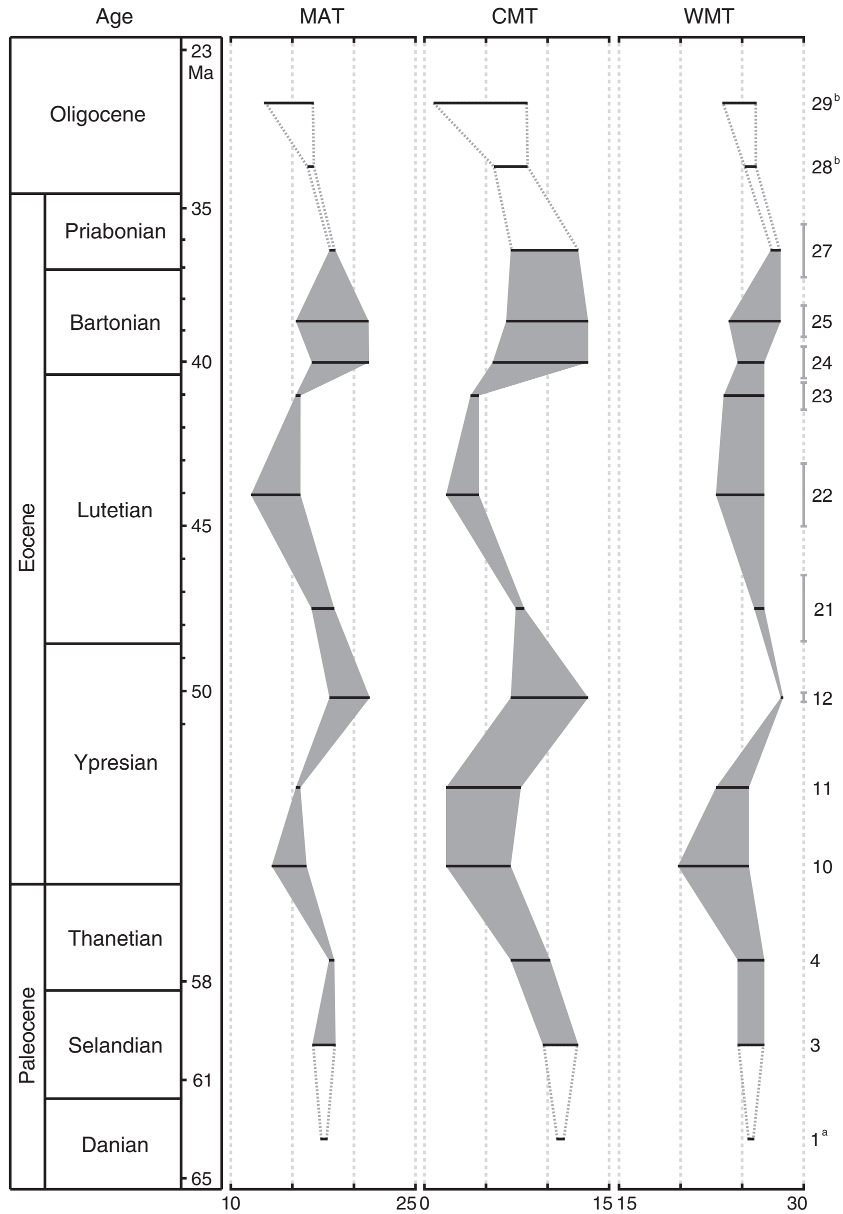

Fig. 5. Temperature variations of northeast China in the Paleogene. The temperature curves were made from the data mainly from Site 2 where it represents the only site in the study with continuous strata ranging from mid Paleocene to upper Eocene. The missing lower Paleocene and Oligocene temperatures for plotting the diagram are converted through our estimated gradients from Sites 1 and 5, respectively. The vertical and horizontal bars as in Fig. 4, and code numbers as in Tables 3 and 4. [a] Temperature parameters converted from the early Paleocene of Jiayin (Site 1, Assemblage 1); [b] Converted from the Oligocene of Shulan (Site 5, Assemblages 28 and 29).

Eocene temperature gradients are believed to be similar to those of the Oligocene (Wei and Wise, 1990; Zachos et al., 1994), the Oligocene temperature condition of Fushun is calculated from Shulan by using the Eocene gradients. The inferred early Oligocene MAT, CMT, and WMT of Fushun are about 16.2–16.7 °C, 5.6–8.4 °C, and 25.3–26.2 °C, respectively, and 11.0–21.4 °C, 0.5–13.9 °C, and 23.4–28.7 °C for the late Oligocene (Fig. 5).

As illustrated in Fig. 5, the WMT appears relatively less sensitive to the climatic fluctuations. On the contrary, the CMT seems to correlate with the MAT, showing highly synchronous variations throughout the Paleogene (Table 4; Fig. 5). A series of climatic changes have been observed during the Paleogene (Fig. 4). The general pattern of Paleogene MAT variations generally matches that derived from marine data (Fig. 4; Fig. 2b in Zachos et al., 2008). The results, based on plant fossils from central Europe, also demonstrate a very similar climatic trend during the mid Eocene to Oligocene (Fig. 3 in Mosbrugger et al., 2005; Fig. 3 in Utescher et al., 2009).

Mosbrugger et al. (2005) reconstructed central European paleoclimates from the late Eocene to Pleistocene, in which the estimated MAT and CMT declined by about 3.5 °C and 9.5 °C, but the corresponding WMT is rather steady. The same patterns of the late Eocene–Oligocene climates have been detected in northeast China (Assemblages 23–25, 27–29 in Fig. 5). Combining the data from central Europe and NE Asia, it appears that the climate cooling of Eurasia during this interval should have mainly originated from intensified winters.

6. Conclusions

The climates throughout the NE Chinese Paleogene are quantitatively reconstructed on the basis of 29 plant assemblages from 8 sites with independent age controls. Our results demonstrate a shallow MAT gradient (0.27 °C/1° latitude) in the NE Chinese Paleocene. During the Eocene, seasonal variations are substantially indicated by apparent differences in annual climate distribution and geographical location of the sites. These variations might imply the early effect of the paleo-East Asian monsoon. Regarding the climate evolution, our results demonstrate that climates of the NE Chinese Paleogene share a generally comparable trend with those of marine records despite the appearance of distinction, and show a similar pattern and corresponding variation magnitudes with those of Europe in the mid Eocene to Oligocene interval. The mean annual temperature declined overall from a warm Paleocene and Eocene to a moderate Oligocene, punctuated by two significant cooling events in the early and mid Eocene, respectively, with a similar magnitude of those continental results from Europe and North America. The mean annual temperature rebounded in the late mid Eocene and then decreased in the Oligocene.

Supplementary materials related to this article can be found online at doi:10.1016/j.palaeo.2011.10.016.

Acknowledgements

Funding for this research was provided by NSFC 41002004 and 41172008, and CPSF 2010603 to C.Q., and NSF EAR-0746105 to Y.S.L. We thank Dr. C. Zhao (Exploration and Development Research Institute, Daqing Oilfield Co. Ltd.) for providing his field notes and original paleogeomagnetic data, Dr. F. Shi (Jilin University) for sharing unpublished geochemical dating results, and Dr. D.H. Wang (Jilin University) for assistance in field work. We are also grateful to Drs. P. Kershaw (Monash University) and T.J. Jones (ETSU), and two anonymous reviewers for their helpful comments.

References

Bice, K.L., Arthur, M.A., Marincovich Jr., L., 1996. Late Paleocene Arctic Ocean shallow-marine temperatures from mollusc stable isotopes. Paleoceanography 11, 241–249.

Bijl, P.K., Schouten, S., Sluijs, A., Reichart, G.-J., Zachos, J.C., Brinkhuis, H., 2009. Early Palaeogene temperature evolution of the southwest Pacific Ocean. Nature 461, 776–779.

Bruch, A.A., Utescher, T., Mosbrugger, V., 2011. Precipitation patterns in the Miocene of Central Europe and the development of continentality. Palaeogeography, Palaeoclimatology, Palaeoecology 304, 202–211.

Chen, B.L., 1985. Tertiary pollen assemblages from Yilan-Yitong area and their stratigraphical significance. Journal of Daqing Petroleum Institute 3, 50–59 (in Chinese with English abstract).

Crowley, T.J., Short, D.A., North, G.R., Mengel, J.G., 1986. Role of seasonality in the evolution of climate during the last 100 million years. Science 231, 579–584.

Davies-Vollum, K.S., 1997. Early Palaeocene palaeoclimatic inferences from fossil floras of the western interior, USA. Palaeogeography, Palaeoclimatology, Palaeoecology 136, 145–164.

Eldrett, J.S., Greenwood, D.R., Harding, I.C., Huber, M., 2009. Increased seasonality through the Eocene to Oligocene transition in northern high latitudes. Nature 459, 969–973.

Fan, M., 1985. Spore-pollen assemblages of Paleocene Xinancun formation in Shulan Coalfield. Coal Technology of Northeast China (3), 13–26 (in Chinese).

Greenwood, D.R., Wing, S.L., 1995. Eocene continental climates and latitudinal temperature gradients. Geology 23, 1044–1048.

Greenwood, D., Wilf, P., Wing, S., Christophel, D., 2004. Paleotemperature estimation using leaf-margin analysis: is Australia different? Palaios 19, 129–142.

Greenwood, D.R., Basinger, J.F., Smith, R.Y., 2010. How wet was the Arctic Eocene rain forest? Estimates of precipitation from Paleogene Arctic macrofloras. Geology 38, 15–18.

Guo, S.X., Zhang, G.F., 2002. Oligocene Sanhe flora in Longjing County of Jilin, Northeast China. Acta Palaeontologica Sinica 41, 193–210 (Suppl.).

Hao, H., Ferguson, D.K., Feng, G.P., Ablaev, A., Wang, Y.F., Li, C.S., 2010. Early Paleocene vegetation and climate in Jiayin, NE China. Climatic Change 99, 547–566.

He, C.X., Tao, J.R., 1997. A study on the Eocene flora in Yilan County, Heilongjiang. Acta Phytotaxonomica Sinica 35, 249–256 (in Chinese with English abstract).

Hong, Y.C., Yang, Z.Q., Wang, S.T., Sun, X.J., Du, N.Q., Sun, M.R., Li, Y.G., 1980. A Research on the Strata and Palaeontology of the Fushun Coal Field in Liaoning Province. Science Press, Beijing. (in Chinese).

Huang, Q.H., Huang, F.T., Zhang, Y., Chen, C.R., Kong, H., Jin, X.X., 1998. New advance in the Tertiary strata study of the Tangyuan Rift. Journal of Stratigraphy 22, 73–80 (in Chinese with English abstract).

Huber, M., Caballero, R., 2011. The early Eocene equable climate problem revisited. Climate of the Past 7, 603–633.

Huber, M., Goldner, A., 2011. Eocene Monsoons. Journal of Asian Earth Sciences. doi:10.1016/j.jseaes.2011.09.014.

Johnson, E.A., 1990. Geology of the Fushun coalfield, Liaoning Province, People's Republic of China. International Journal of Coal Geology 14, 217–236.

Jolley, D.W., Widdowson, M., 2005. Did Paleogene North Atlantic rift-related eruptions drive early Eocene climate cooling? Lithos 79, 355–366.

Li, D.J. (Ed.), 1997. Stratigraphy (Lithostratic) of Jilin Province. : Multiple Classification and Correlation of the Stratigraphy of China, vol. 22. China University of Geosciences Press, Wuhan (in Chinese with English abstract).

Liu, M.L., 1987. Early Tertiary palynological assemblages of Hunchun Coal-field, Jilin Province. Professional Papers Stratigraphy Palaeontology 17, 167–192 (in Chinese).

Liu, M.L., 1990. The Eocene spore pollen assemblages from the Dalianhe Formation, Yilan Coal-field, Heilongjiang Province. Bulletin of the Shenyang Institute of Geology and Mineral Resources, Chinese Academy of Geological Sciences 20, 111–137 (in Chinese with English abstract).

Liu, Y.S., Guo, S.X., Ferguson, D.K., 1996. A catalogue of Cenozoic megafossil plants in China. Palaeontographica Abteilung B: Paläophytologie 238, 141–179.

Liu, Y.S., Utescher, T., Zhou, Z., Sun, B., 2011. The evolution of Miocene climates in North China: preliminary results of quantitative reconstructions from plant fossil records. Palaeogeography, Palaeoclimatology, Palaeoecology 304, 308–317.

Manchester, S.R., Chen, Z.D., Geng, B.Y., Tao, J.R., 2005. Middle Eocene flora of Huadian, Jilin Province, Northeastern China. Acta Palaeobotanica 45, 3–26.

Mosbrugger, V., Utescher, T., 1997. The coexistence approach—a method for quantitative reconstructions of Tertiary terrestrial palaeoclimate data using plant fossils. Palaeogeography, Palaeoclimatology, Palaeoecology 134, 61–86.

Mosbrugger, V., Utescher, T., Dilcher, D.L., 2005. Cenozoic continental climatic evolution of Central Europe. Proceedings of the National Academy of Sciences of the United States of America 102, 14964–14969.

Pearson, P.N., van Dongen, B.E., Nicholas, C.J., Pancost, R.D., Schouten, S., Singano, J.M., Wade, B.S., 2007. Stable warm tropical climate through the Eocene Epoch. Geology 35, 211–214.

Peppe, D.J., Royer, D.L., Cariglino, B., Oliver, S.Y., Newman, S., Leight, E., Enikolopov, G., Fernandez-Burgos, M., Herrera, F., Adams, J.M., Correa, E., Currano, E.D., Erickson, J.M., Hinojosa, L.F., Hoganson, J.W., Iglesias, A., Jaramillo, C.A., Johnson, K.R., Jordan, G.J., Kraft, N.J.B., Lovelock, E.C., Lusk, C.H., Niinemets, Ü., Peñuelas, J., Rapson, G., Wing, S.L., Wright, I.J., 2011. Sensitivity of leaf size and shape to climate: global patterns and paleoclimatic applications. New Phytologist 190, 724–739.

Qu, S., 1993. Characteristic and its geological significance of the palynological assemblege of the Lower Tertiary Genjiajie Group in Fushun Basin. Journal of Changchun University of Earth Sciences 23, 411–415 (in Chinese with English abstract).

Quan, C., Zhang, L., 2005. An analysis of the Early Paleogene climate of the Jiayin Area, Heilongjiang province. Geological Review 51, 10–15 (in Chinese with English abstract).

Quan, C., Liu, Y.S., Utescher, T., 2011. Paleogene evolution of precipitation in northeast China supporting the middle Eocene intensification of the East Asian monsoon. Palaios 26, 743–753.

Roberts, C.D., LeGrande, A.N., Tripati, A.K., 2009. Climate sensitivity to Arctic seaway restriction during the early Paleogene. Earth and Planetary Science Letters 286, 576–585.

Rohli, R.V., Vega, A.J., 2008. Climatology. Jones and Bartlett Publishers, Sudbury, Massachusetts.

Shao, J.A., Zhang, L.Q., Xiao, Q.H., Li, X.B., 2005. Rising of Da Hinggan Mts in Mesozoic: a possible mechanism of intracontinental orogeny. Acta Petrologica Sinica 21, 789–794 (in Chinese with English abstract).

Shellito, C.J., Sloan, L.C., 2006. Reconstructing a lost Eocene paradise: Part I. Simulating the change in global floral distribution at the initial Eocene thermal maximum. Global and Planetary Change 50, 1–17.

Shi, F., Xin-rong, Z., Zhao-jun, L., He-yong, W., Jian-guo, Y., 2008a. Thrust event of the provenances revealed by zircon fission track ages in Tangyuan Fault-Basin, NE China. Radiation Measurements 43, S324–S328.

Shi, Y.Z., Liu, Z.J., Liu, R., Du, J.F., Zhang, J., Liu, P., 2008b. Quantitative reconstruction of the Eocene palaeoclimate in the Fushun Basin, Liaoning Province. Journal of Jilin University (Earth Science Edition) 38, 50–55 (in Chinese with English abstract).

Sloan, L.C., Barron, E.J., 1992. A comparison of Eocene climate model results to quantified paleoclimatic interpretations. Palaeogeography, Palaeoclimatology, Palaeoecology 93, 183–202.

Song, Z., Zheng, Y., Li, M., Zhang, Y., Wang, W., Wang, D., Zhao, C., Zhou, S., Zhu, Z., Zhao, Y., 1999. Late Cretaceous and Tertiary Spores and Pollen. Fossil spores and pollen of China, vol. 1. Science Press, Beijing (in Chinese).

Spicer, R.A., Bera, S., De Bera, S., Spicer, T.E.V., Srivastava, G., Mehrotra, R., Mehrotra, N., Yang, J., 2011. Why do foliar physiognomic climate estimates sometimes differ from those observed? Insights from taphonomic information loss and a CLAMP case study from the Ganges Delta. Palaeogeography, Palaeoclimatology, Palaeoecology 302, 381–395.

Stap, L., Lourens, L.J., Thomas, E., Sluijs, A., Bohaty, S., Zachos, J.C., 2010. High-resolution deep-sea carbon and oxygen isotope records of Eocene Thermal Maximum 2 and H2. Geology 38, 607–610.

Su, T., Xing, Y.W., Yang, Q.S., Zhou, Z.K., 2009. Reconstructions of mean annual temperature in Chinese Eocene paleofloras based on leaf margin analysis. Acta Palaeontologica Sinica 48, 65–72 (in Chinese with English abstract).

Su, T., Xing, Y.W., Liu, Y.S., Jacques, F.M.B., Chen, W.Y., Huang, Y.J., Zhou, Z.K., 2010. Leaf margin analysis: a new equation from humid to mesic forests in China. Palaios 25, 234–238.

Sun, G., Quan, C., Sun, C.L., Sun, Y.W., Luo, K.L., Lu, J.S., 2005. Some new knowledge on subdivisions and age of Wuyun Formation in Jiayin of Heilongjiang, China. Journal of Jilin University (Earth Science Edition) 35, 137–142 (in Chinese with English abstract).

Tripati, A., Zachos, J., Marincovich, L., Bice, K., 2001. Late Paleocene Arctic coastal climate inferred from molluscan stable and radiogenic isotope ratios. Palaeogeography, Palaeoclimatology, Palaeoecology 170, 101–113.

Utescher, T., Mosbrugger, V., 1997–2011. PALAEOFLORA Database. http://www.palaeoflora.de/1997–2011.

Utescher, T., Djordjevic-Milutinovic, D., Bruch, A., Mosbrugger, V., 2007. Palaeoclimate and vegetation change in Serbia during the last 30 Ma. Palaeogeography, Palaeoclimatology, Palaeoecology 253, 141–152.

Utescher, T., Mosbrugger, V., Ivanov, D., Dilcher, D.L., 2009. Present-day climatic equivalents of European Cenozoic climates. Earth and Planetary Science Letters 284, 544–552.

Utescher, T., Bruch, A.A., Micheels, A., Mosbrugger, V., Popova, S., 2011. Cenozoic climate gradients in Eurasia—a palaeo-perspective on future climate change? Palaeogeography, Palaeoclimatology, Palaeoecology 304, 351–358.

Wang, Q., Ferguson, D.K., Feng, G.P., Ablaev, A.G., Wang, Y.F., Yang, J., Li, Y.L., Li, C.S., 2010. Climatic change during the Palaeocene to Eocene based on fossil plants from Fushun, China. Palaeogeography, Palaeoclimatology, Palaeoecology 295, 323–331.

Wei, W., Wise Jr., S.W., 1990. Biogeographic gradients of middle Eocene–Oligocene calcareous nannoplankton in the South Atlantic Ocean. Palaeogeography, Palaeoclimatology, Palaeoecology 79, 29–61.

Whittaker, R.H., 1975. Communities and ecosystems. MacMillan, New York.

Wilf, P., 2000. Late Paleocene-early Eocene climate changes in southwestern Wyoming: paleobotanical analysis. Geological Society of America Bulletin 112, 292–307.

Wing, S.L., Greenwood, D.R., 1993. Fossils and fossil climates: the case for equable continental interiors in the Eocene. Philosophical Transactions of the Royal Society B: Biological Sciences 341, 243–252.

Wing, S.L., Harrington, G.J., 2001. Floral response to rapid warming in the earliest Eocene and implications for concurrent faunal change. Paleobiology 27, 539–563.

Wing, S.L., Bao, H., Koch, P.L., 2000. An early Eocene cool period? Evidence for continental cooling during the warmest part of the Cenozoic. In: Huber, B.T., MacLeod, K.G., Wing, S.L. (Eds.), Warm Climates in Earth History. Cambridge University Press, Cambridge, pp. 197–237.

Wing, S.L., Harrington, G.J., Smith, F.A., Bloch, J.I., Boyer, D.M., Freeman, K.H., 2005. Transient floral change and rapid global warming at the Paleocene–Eocene boundary. Science 310, 993–996.

Wolfe, J.A., 1993. A method of obtaining climatic parameters from leaf assemblages. U.S. Geological Survey Bulletin 2041, 1–71.

Woodburne, M.O., Gunnell, G.F., Stucky, R.K., 2009. Climate directly influences Eocene mammal faunal dynamics in North America. Proceedings of the National Academy of Sciences of the United States of America 106, 13399–13403.

Wu, C., Wang, X., Liu, G., Li, S., Mao, X., Li, X., 2002. Study on dynamics of tectonic evolution in the Fushun Basin, Northeast China. Science in China Series D: Earth Sciences 45, 311–324.

Yang, X.D., Li, X.Y. (Eds.), 1997. Stratigraphy (Lithostratic) of Liaoning Province. : Multiple Classification and Correlation of the Stratigraphy of China, vol. 21. China University of Geosciences Press, Wuhan (in Chinese with English abstract).

Yang, J.G., Huang, Q.H., Wu, C.D., Wu, H.Y., 2004. Sequences and ages of the Paleogene and Neogene strata in the Tangyuan Rift, Heilongjiang. Journal of Stratigraphy 28, 168–172 184 (in Chinese with English abstract).

Zachos, J.C., Stott, L.D., Lohmann, K.C., 1994. Evolution of Early Cenozoic marine temperatures. Paleoceanography 9, 353–387.

Zachos, J.C., Dickens, G.R., Zeebe, R.E., 2008. An early Cenozoic perspective on greenhouse warming and carbon-cycle dynamics. Nature 451, 279–283.

Zhang, Y., Wang, K., Wang, J., 1987. Pollen assemblages from Hunchun Coalmine of Hunchun, Jilin Province and its paleovegetational and paleoclimatic significance. Coal Geology & Exploration 1, 18–25 (in Chinese with English abstract).

Zhang, F., Wang, K.W., Liu, L., 2007a. Stratigraphic sequence of Neogence system in Yi-Shu graben. Journal of Jilin University (Earth Science Edition) 37, 112–119 (in Chinese with English abstract).

Zhang, J.Y., Peng, Y.J., Liu, J., 2007b. An important discontinuity of the Paleogene volcanic incidents in northeast China and their prospecting significance. Jilin Geology 26, 1–7 (in Chinese with English abstract).

Zhang, S.Q., Liu, R.Y., Li, M.S., 2010. Eocene–Miocene palynological assemblages in Wanchang area of Jilin and their stratigraphic significance. Global Geology 29, 357–362 (in Chinese with English abstract).

Zhao, C., Ye, D., Wei, D., Chen, B., Liu, D., 1994. Tertiary in Petroliferous Regions of China. Petroleum Industry Press, Beijing (in Chinese).

Zhou, Z.Y., Wu, X.W. (Eds.), 2002. Chinese Bibliography of Palaeobotany (Megafossils) (1865–2000). University of Science and Technology of China Press, Hefei (in Chinese and English).